Supplement Material

In Situ Hybridization

Whole-mount *in situ* hybridization was carried out as previously described [1]. Digoxigenin-labeled RNA probes were prepared by *in vitro* transcription. The full-length cDNA for murine *Zac1* (accession no. AK142210) was obtained by RT-PCR and subcloned into the pBluescript plasmid. The cDNAs for murine Nkx2-5, GATA4, ANP, MLC2-v, and MLC-2a were kindly provided by Dr. E.N. Olson and Dr. H. Yamagishi. The probes were transcribed with T3 or T7 RNA polymerase.

Animal study

Pregnant ICR wild-type mice were purchased from Japan CLEA. All experiments were approved by the Keio University Ethics Committee for Animal Experiments.

Immunostaining

Antibodies directed against Zac1 (G-18; Santa Cruz Biotechnology, Santa Cruz, CA), actinin (EA-53; Sigma, St. Louis, MO), Lamin A/C (#2032, Cell Signaling Technology), Rho-GDI (610255, BD Biosciences), phospho-histone H3 (9071; Cell Signaling) and phalloidin (Molecular Probes, Eugene, OR) were added to the sections, followed by overnight incubation at 4°C. Next, three 5-min washes in PBS were carried out, followed by the addition of secondary antibodies conjugated with Alexa 546 (Molecular Probes), and incubation for 1 h at room temperature. The sections were washed three times in PBS for 5 min each and then observed by confocal laser-scanning microscopy (LSM510; Carl Zeiss, Jena, Germany). The TUNEL assay was performed using the ApopTag Red In Situ Apoptosis Detection kit (Chemicon International) according to the manufacturer's protocol.

Western blotting

COS7 cells were transfected with pcDNA3.1 Zac1 using Lipofectamine (Invitrogen, Carlsbad, CA). Cell extracts were isolated 24 h after transfection and separated into nuclear and cytosolic fractions. Fractionated protein lysates were resolved by SDS-PAGE and transferred to a PVDF membrane, followed by immunoblotting with rabbit anti-Zac1 antibody (Santa Cruz Biotechnology) at a dilution of 1:1,000 and horseradish peroxidase-conjugated anti-goat IgG, followed by development with the SuperSignal West Pico Chemiluminescent reagent (Pierce, Rockford, IL).

IP-western blot analysis

Total cell lysate was prepared from neonatal mouse hearts. IP-western blot analysis was performed essentially as described previously using anti-Zac1 and anti-Nkx2-5 for hearts lysate.

Plasmids

The Zac1-expressing plasmids were generated through conventional or PCR-based cloning. Deletion mutants were constructed by PCR-based mutagenesis and subcloning of the DNA fragments into the pcDNA3.1 expression vector. Site-directed mutagenesis was performed using the QuickChange kit (Stratagene, La Jolla, CA). The reporter plasmids (ANP-luciferase, BNP-luciferase, and α-MHC-luciferase) were kindly provided from Dr. E.N. Olson. The *Zac1* promoter was cloned using PCR-based techniques from a BAC clone into the pGL3 basic vector (Promega, Madison, WI). For mammalian hybrid assay, pBIND vector and pG5luc vector were purchased from Promega.

Cell culture, transfection, and luciferase assay

COS-7 cells plated in DMEM with 10% FBS were transfected with Lipofectamine (Invitrogen) according to the manufacturer's instructions. Unless otherwise indicated, 100ng of reporter and 100ng of each activator plasmid were used. The DNA doses represented by the ramp symbol indicate 0, 30, 100 and 300ng of plasmid. The total amount of DNA per well was kept constant by adding the corresponding amount of expression vector without a cDNA insert. CMV-*Renilla* luciferase was used as an internal control, to normalize for variations in transfection efficiency. All the proteins were expressed at very similar levels, as confirmed by Western blotting.

EMSA

Nuclear extracts were collected from COS7 cells that overexpressed Zac1. Double-stranded oligonucleotides for the Zac1-binding sequence '(5 -GCATCTTCTGCTGGCCGCCG-3') were synthesized, and the two complementary oligonucleotides were annealed and labeled with [α-^{32}P]-dATP using the Klenow enzyme. Labeled probes were incubated with 5 ml of nuclear extracts and 2mg of poly(dI-dC) in 20 ml of binding buffer [10 mM Tris-HCl (pH 7.5), 50 mM NaCl, 10% glycerol, 0.5 mM dithiothreitol, 0.05% Nonidet P-40] for 30 min at room temperature. The protein/DNA mixture was resolved on a 5% polyacrylamide gel in 0.5 Tris borate/EDTA buffer at 4°C for 2 h at 150 V.

ChIP assay

For the *in vivo* ChIP experiments, extracts were prepared from five neonatal rat wild-type hearts for independent experiments. For the ChIP assays, we used the Chromatin Immunoprecipitation Assay Kit (Upstate Biotechnology, Lake Placid, NY) and followed the instructions of the supplier. Primer in PCR reactions is 5'-ACAAGCTTCGCTGGACTGAT-3' and 5'-TCTCGGCTCACTCTCTGGTT-3' (-148 +43), 5'-CCTGACTGCTAACAGGGACA-3' and 5'-

TGTCAGGGGCTCCAAATAAG-3′ (-576 -398), 5′-GAGAGGAGCTGGACCATGAG-3′ and 5′-TTGAAAGCGTGAGGACTTGA-3′ (-2907 -2728). The amplified region corresponded to the rat ANP promoter, which encompasses the Zac1-binding sites.

Glutathione S-transferase (GST) pulldown assay

Murine Zac1 cDNA and several DNA fragments encoding Zac1 were subcloned into the pGex-6P vector (Amersham Biosciences). GST fusion proteins were isolated by standard procedures. The plasmids that contained the deletion mutants of Nkx2-5 were gifted by Dr. I. Komuro. Proteins translated *in vitro* were labeled with [^{35}S]-methionine in the coupled transcription-translation T7 reticulocyte lysate system (Promega), and assayed for binding to the GST-fusion proteins.

RT-PCR and real-time quantitative PCR

Total RNA was extracted using the Trizol reagent (Invitrogen), and RT-PCR was performed as described previously. At least five replicates were processed for each assay. *GAPDH* was used as an internal control. For quantitative analysis of *Nkx2-5*, *GATA4*, *ANP*, *MLC2v*, and *MLC2a* expression, the respective cDNA was used as the template in a TaqMan real-time PCR assay using the ABI Prism 7700 sequence detection system (Applied Biosystems) according to the manufacturer's instructions. All samples were run in triplicate. The data were normalized to *GAPDH* expression. The primers and TaqMan probe for *Nkx2-5*, *GATA4*, *ANP*, *MLC2v*, *MLC2a* and *Zac1* were Mm00657783_m1, Mm00484689_m1, Mm01255747_g1, Mm00440384_m1, Mm00491655_m1, and Mm00494251_m1, respectively.

Generation of mutant mice

The *Zac1*-mutated mice were generated by Lexicon Pharmaceuticals from ES cells that corresponded to OST181461 (OmniBank sequence tag) and that were targeted by gene trapping. The gene-trapping vector contained a retroviral 5 -end long terminal repeat (LTR), a splice acceptor sequence, neomycin gene (Neo), and partial first intron of the murine *Bruton's tyrosine kinase* (*Btk*) gene as the 3 -trapping component, rather than a selectable marker, which was regulated by the 3-phosphoglycerate kinase 1 (PGK-1) gene promoter, a splice donor sequence, and a 3′-LTR[2]. Retroviral infection, selection, and screening of the ES cells were performed as previously described. The gene-trapping vector was inserted at the third intron of the *Zac1* gene (corresponding to OST181461) in the ES cells, as detected by inverse-PCR. ES cells were selected for blastocyst injection into C57BL/6 mice to produce chimeric mice. Heterozygous and homozygous animals were analyzed along with littermate control animals.

Statistical Analyses

Values are presented as mean ± SEM. Statistical significance was evaluated with the unpaired Student *t* test for comparisons between 2 mean values. A chi squared analysis for comparisons between 2 groups. Comparisons between >3 groups were performed with ANOVA. A value of $P<0.05$ was considered significant. *p<0.05, **P<0.01, NS; not significant.

References

1. Yuasa S, Itabashi Y, Koshimizu U, Tanaka T, Sugimura K, Kinoshita M, Hattori F, Fukami S, Shimazaki T, Ogawa S, Okano H, Fukuda K. Transient inhibition of BMP signaling by Noggin induces cardiomyocyte differentiation of mouse embryonic stem cells. *Nat Biotechnol.* 2005;23:607-611.

2. Zambrowicz BP, Friedrich GA, Buxton EC, Lilleberg SL, Person C, Sands AT. Disruption and sequence identification of 2,000 genes in mouse embryonic stem cells. *Nature.* 1998;392:608-611.

Supplement Material

Online Figure I

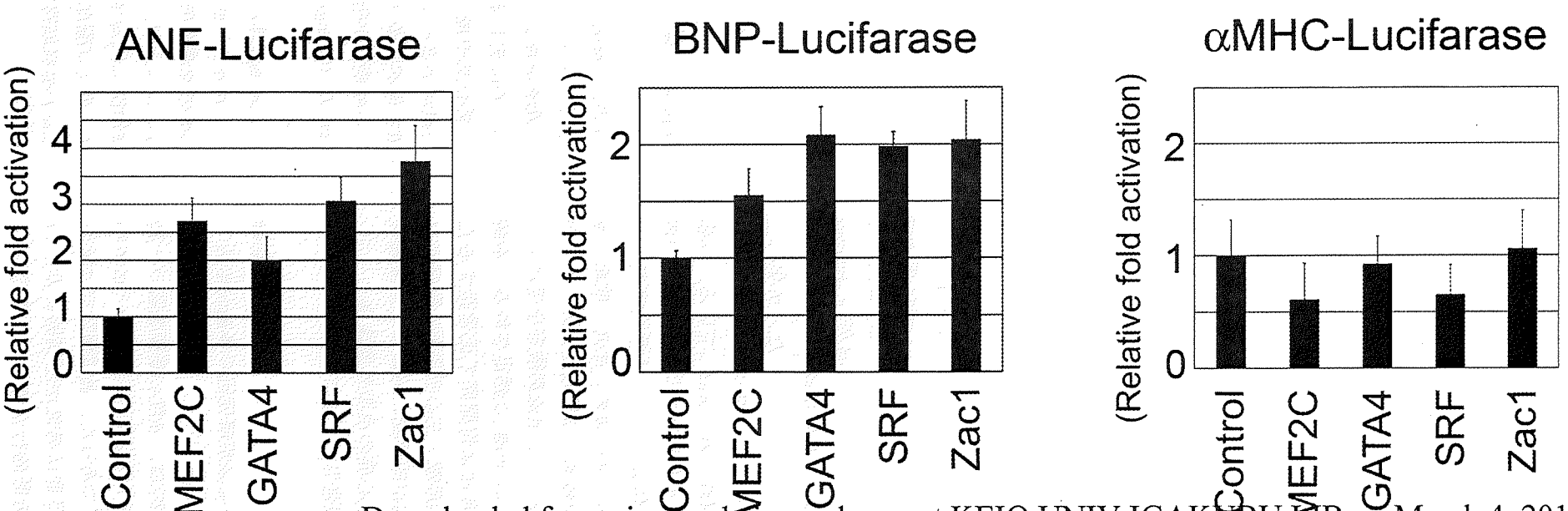

注目されている病態，疾患の診断と治療

たこつぼ心筋症の診断と治療

河合祥雄

順天堂大学医学部循環器内科／かわい・さちお

はじめに

たこつぼ心筋症(たこつぼ心筋障害 Takotsubo (ampulla) cardiomyopathy)とは，急性発症の原因不明の左心室心尖部バルーン状拡張(無収縮)を呈する症例をいう[1]．心尖部の無収縮は数週～1ヵ月以内に大部分の症例では，ほぼ正常化する．本疾患がわが国の心臓専門医に普く知れわたったのは，佐藤らによる「たこつぼ」の名称が冠された1990年代以降で，それ以降，国内では日常診療レベルの疾患となった．本病態が日本人以外にもあると欧米で理解されたのは，2003年のDesmetらの報告以降である．本病態は最近に発生した病態ではなく，古くから存在していた．25年以上も前に，時岡ら[2]は心エコー図で，心尖部を含む心室の可逆的な収縮低下例を検討している．本症例がわが国で先駆けて発見されたのは，日本の医療事情(国民皆保険制度下における低検査料・低手術料，冠動脈介入治療の進歩と普及，検査・施術年齢の引き上げの結果，急性冠症候群の多くが早期に冠状動脈造影・左心室造影検査を受けている事実)がもたらした「幸運」と想定される．本病態の左心室壁運動異常は短期間で正常化するため，超急性期の冠状動脈・左心室造影の観察がなければ，左心室機能が短期間に回復した正常冠状動脈症例または気絶心筋の典型的臨床例として，今まで認識され，報告されてきていた．

頻　度

厚生労働省特発性心筋症研究班の多施設全国アンケート調査(2000年8月)で，実数提示施設に限定した頻度(有病率)は，急性心筋梗塞疑い・緊急冠状動脈造影症例の施設間平均2.3％(粗平均1.4％：96/6,774例)であった．通常施設では緊急冠状動脈造影施行患者は男性が圧倒的に多いので，緊急冠状動脈造影施行女性患者に限定すれば，本病態の頻度は2.3％の数倍(8％ほど)に当たると推定される．

症　状

当初，急性冠症候群に類似の胸痛で発症すると記載され，理解されていたが，最近は急性発症の呼吸困難や無症状発症例も少なくないことが判明している．

病　態

たこつぼ心筋障害の病態として以下のことが注目されている．

心尖部のバルーン状の無収縮と心基部過収縮を特徴とするが，心基部過収縮の頻度は必ずしも高くない．心基部過収縮，すなわち心室流出路機能性狭窄(圧較差，血流速度亢進，心雑音)は3割から1割程度(同一施設連続11例中4例，72例中12例)の頻度で観察される．左心室のみならず右心室にもみられる．閉塞性肥大型心筋症の閉塞とは機序が異なり，流出路心筋が括約筋様に収縮するために生じる可能性が考えられる．本症ではS字型心室中隔(sigmoid septum)をもち，左心室容量が小さいヒト(主に女性)が強力な交感試験刺激や脱水に曝された場合に左心室流出路障害が生じる可能性が指摘されている．たこつぼ心筋障害例におけるsigmoid septumの頻度は明らかではない．

心尖部以外にさまざまな部位に収縮異常をみることがあり，逆たこつぼ，心室中部バルーニング，局所的壁運動異常などの非典型例はおよそ4割ともいわれるが，母集団に，脳血管障害を含めるか，特発性に限局するかでその値は異なる．実際には，例えば脳血管障害や褐色細胞腫crisisにみられる心室収縮障害ではさまざまな部位に収縮異常をみる．

0910-1551/09/¥100/頁/JCOPY

◎たこつぼ心筋症(心筋障害)は最近に発生した病態ではない.
◎気絶心筋の典型例と誤認されることが多く,
高齢女性の緊急冠状動脈造影施行の8%ほどにあたる.
◎必ずしも発生契機にストレスはなく,また無症状での発症がある.

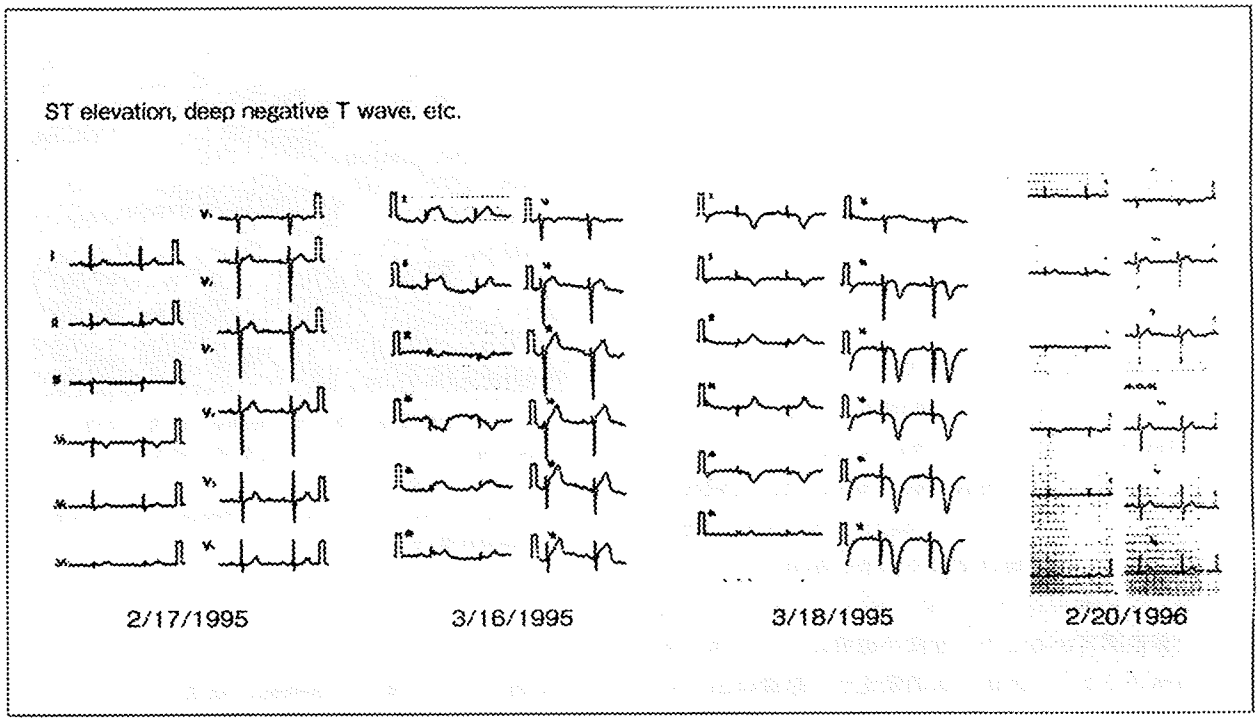

図1 心電図経過(60歳,女性)

高齢者ことに高齢女性に多発する(男性の7倍).多くの症例で,情動ストレス(女性では精神的ストレス,男性では肉体的なストレス優位)が誘因もしくは契機に発症することが知られる.アメリカ心臓協会の新しい心筋症分類では,stress cardiomyopathyとも呼ばれるが,明らかな契機なしに発症する症例も確実に存在するので,ストレス心筋症との名称は成因論的にも適切ではあり得ない.最近では大地震などの自然災害時の発症も注目を集めている.

検査所見◉

心電図

発症直後にST上昇がみられる.冠攣縮による

ST上昇より長い持続時間をもつ.持続に関しての記載のある症例では2時間,24時間,翌日までが各1例,2週間持続が2例ある.対側性変化が欠如する場合がある.少数例で急性期に異常Q波やQRS電位差の変化(胸部誘導のinitial R波の減高)を認めることもある.その後,典型例では広範な誘導でT波が陰転(巨大陰性T波)し,次第に陰性部分が深くなり,QT延長を伴う.大多数で広汎前壁(前側壁)中隔梗塞を示す誘導部位でのST上昇がみられているが,広範・巨大陰性T波のみを記載している症例もある.本症の経時的変化ではST上昇の後に陰性T波に移行するので,初診時期の問題もあると思われる.陰性T波の回復にはより長期を要し,しかも,個体差が

◎心筋障害は早期は細胞浸潤，次いで心筋脱落，巣状の線維症との経時的変化が想定される．
◎障害心筋細胞数は心基部より心尖部で多く，死亡までの時期により，障害心筋細胞は処理される．

みられる．この時期が長いので，所見としては最も多い．この変化は徐々に回復するが，陰性T波は数ヵ月続き，年余にわたる例がある(図1)．

心筋逸脱酵素は典型例においては，実際の心筋障害程度を反映して，急性心筋梗塞や劇症心筋炎に比較し，すなわち，壁運動低下に釣り合わない低値(中程度以下)に留まる．血中カテコラミン上昇例がある．または上昇を欠如する例がある．

冠状動脈造影は急性期に行うことが望ましいが，典型例では急性心筋梗塞との鑑別がさほど困難でない(高齢女性，心電図異常経過，逸脱酵素値低値などから)ので，慢性期造影でよいとする意見も多い．冠状動脈攣縮誘発率は低く自験例で約1/3．Tsuchihashiらの論文[3]では21％に過ぎず，しかも冠攣縮誘発時に心室収縮異常を再現し得たとの報告はない．flow wire studyで冠血流予備能異常があるが，冠微小循環における異常を意味するが，主因か二次的変化かの結論は出ていない．

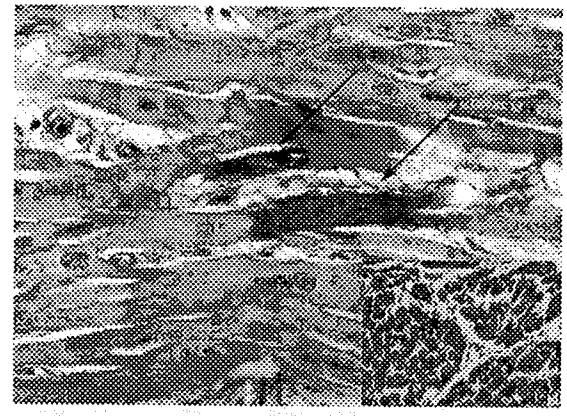

図2　心筋組織像：単一性心筋障害(81歳，女性)
介在板を境界として，個々の心筋細胞が障害されている．左心室中層(HE染色，400倍)
右下：障害は原則として，個々の心筋細胞，もしくは数個の心筋細胞が標的となる．右心室心尖部(アザン染色，200倍)

心筋組織障害◉

心筋組織障害が生じていることは心筋逸脱酵素値の上昇より，容易に推定される事柄であるが，心筋生検を施行した報告は少なく，われわれ以外に剖検例を含めた複数の組織病理所見を詳細に観察した研究はない．

生検例の観察では，早期は細胞浸潤，次いで心筋脱落，巣状の線維症との経時的変化が想定された．心室瘤を後遺する例もある．剖検例では，好酸性染色性の亢進，筋収縮帯形成，融解などの単一心筋細胞障害像(図2)，それらの集簇像，および心筋細胞に対する細胞反応もしばしば認められた．剖検例では心基部と心尖部の病変程度が異なり，障害心筋細胞数は心基部より心尖部で多く，心尖部～前壁の壁運動低下を説明した．死亡までの時期により，障害心筋細胞は処理されていた．

成　因◉

本病態は，当初は多枝攣縮による気絶心筋の臨床例と考えられたが，虚血が証明されておらず，心筋気絶の定義に合致しない．この心筋気絶説・心筋循環障害(攣縮)説は，慢性期の低冠攣縮誘発率(1/3例以下)，心筋障害・壊死像および一過性の左右心室流出路閉塞の説明が困難であることより，否定的である．その他に，心筋微小循環障害があり，心筋内の冠血流測定で所見が明らかにされている．しかし，心筋微小循環障害が一時的に広範な心尖部収縮不全を起こし，心基部を過収縮にする機序の説明は困難であり，二次的な変化である可能性は否定できない．

心筋炎は，本疾患の欧米での最初の報告であるbroken heartのCPCでの病理診断であったが，先行感染欠如，心筋細胞障害の先行，心電図経過，

◎大部分が速やかに回復するが，肺水腫や他の後遺症を呈する例，死亡例がある．
◎本病態は従来注目されていなかった，未知の非虚血性心筋障害である．

回復過程などの諸点から否定的と考える[4]．ただし，カテコラミン心筋炎(カテコラミンによる心筋細胞障害)はその組織像はきわめて本症に酷似しており，心臓自律神経との関連で注目される．

基礎病態にカテコラミン・β刺激薬使用，Guillain-Barré 症候群の存在は，発症における心臓自律神経の異常を推定させる．Ueyama らはラット拘束実験で4割に心尖部バルーニング，4割にびまん性収縮低下を作り，adrenoreceptor 遮断薬前投与で予防[5]しうることを示した．左心室心尖部における交感神経刺激に対する不均一反応が明らかにされ，左心室心尖部における疎な交感神経線維密度を代償する，より高いβ-adrenergic 受容体密度と交感神経刺激に対する高い心筋反応性を有し，これが各種ストレス下での心筋障害・機能低下の成因と考えられている．

予　後

大部分が速やかに回復するが，肺水腫や他の後遺症を呈する例，死亡例がある．重症例は呼吸不全を呈することがある．心室中隔穿孔例や心破裂などでの死亡症例が存在する．10年間のたこつぼ心筋障害死亡例・剖検例の報告抄録，論文に記録された死亡例数は37例で，神経性食思不振症34歳を除く平均76歳(61～90歳)．病期は第1病日から第33病日で平均10日，1週間以内の死亡は15例であった．死因は肺炎，敗血症，MOF などの基礎疾患，心破裂(6例)，心タンポナーデ，心室不整脈．2002年に施行した79施設に対するアンケート調査では618例中25例の死亡(4.04%)，8例(1.3%)の重度後遺症(心室瘤，完全房室ブロック，心不全再発など)があり，計5%は死亡・重度後遺症をもつ．死因としては早期心破裂が重要である．

治　療

β遮断薬が実験的に作成されたカテコラミン誘導性のたこつぼ心筋症モデルに有効との報告はあるが，臨床での比較対照試験はない．

まとめ

本病態は従来注目されていなかった，未知の非虚血性心筋障害であり，呼吸困難，肺水腫，ショックで発症する重症例も存在する．原因不明の突然死の中のストレスと関連する症例の一部を占めている可能性も考えられる．

文　献

1) 河合祥雄：たこつぼ心筋障害(たこつぼ心筋症)の診断の手引き(第2案)作成過程．心臓36：466-468，2004(河合祥雄：たこつぼ心筋障害(たこつぼ心筋症)，北畠　顕ほか編「厚生労働省難治性疾患克服研究事業 特発性心筋症調査研究班 心筋症 診断の手引きとその解説」，かりん社，札幌，p.109-116，2005)
2) 時岡正明ほか：手術後に認められた一過性心筋梗塞様心電図と断層心エコー図上の広汎なアシナジー．J Cardiography 15：639-653，1983
3) Tsuchihashi, K. et al.：Transient left ventricular apical ballooning without coronary artery stenosis：a novel heart syndrome mimicking acute myocardial infarction. J Am Coll Cardiol 38：11-18, 2001
4) 河合祥雄："タコツボ"型心筋症とはどういう疾患か―"タコツボ"型心筋障害疾症説の検討―．心エコー 2(10)：860-865，2001
5) Ueyama, T. et al.：Emotional stress induces transient left ventricular hypocontraction in the rat via activation of cardiac adrenoceptors：a possible animal model of 'tako-tsubo' cardiomyopathy. Circ J 66：712-713, 2002

Am J Physiol Heart Circ Physiol 298: H1072–H1078, 2010.
First published January 15, 2010; doi:10.1152/ajpheart.00255.2009.

Tenascin-C may aggravate left ventricular remodeling and function after myocardial infarction in mice

Tomohiro Nishioka,[1] Katsuya Onishi,[2] Naoshi Shimojo,[1] Yuka Nagano,[1] Hidenori Matsusaka,[3] Masaki Ikeuchi,[3] Tomomi Ide,[3] Hiroyuki Tsutsui,[4] Michiaki Hiroe,[5] Toshimichi Yoshida,[1] and Kyoko Imanaka-Yoshida[1]

Departments of [1]Pathology and Matrix Biology and [2]Laboratory Medicine, Mie University Graduate School of Medicine, Tsu; [3]Department of Cardiovascular Medicine, Graduate School of Medical Sciences, Kyushu University, Fukuoka; [4]Department of Cardiovascular Medicine, Graduate School of Hokkaido University, Sapporo; and [5]Department of Cardiology, International Medical Center of Japan, Tokyo, Japan

Submitted 16 March 2009; accepted in final form 9 January 2010

Nishioka T, Onishi K, Shimojo N, Nagano Y, Matsusaka H, Ikeuchi M, Ide T, Tsutsui H, Hiroe M, Yoshida T, Imanaka-Yoshida K. Tenascin-C may aggravate left ventricular remodeling and function after myocardial infarction in mice. *Am J Physiol Heart Circ Physiol* 298: H1072–H1078, 2010. First published January 15, 2010; doi:10.1152/ajpheart.00255.2009.—Tenascin-C (TN-C) is an extracellular matrix glycoprotein with high bioactivity. It is expressed at low levels in normal adult heart, but upregulated under pathological conditions, such as myocardial infarction (MI). Recently, we (Ref. 34) reported that MI patients with high serum levels of TN-C have a greater incidence of maladaptive cardiac remodeling and a worse prognosis. We hypothesized that TN-C may aggravate left ventricular remodeling. To examine the effects of TN-C, MI was induced by ligating coronary arteries of TN-C knockout (KO) mice under anesthesia and comparing them with sibling wild-type (WT) mice. In WT+MI mice, TN-C expression was upregulated at *day 1*, peaked at *day 5*, downregulated and disappeared by *day 28*, and the molecule was localized in the border zone between intact myocardium and infarct lesions. The morphometrically determined infarct size and survival rate on *day 28* were comparable between the WT+MI and KO+MI groups. Echocardiography and hemodynamic analyses demonstrated left ventricular end-diastolic diameter, myocardial stiffness, and left ventricular end-diastolic pressure to be significantly increased in both WT+MI and KO+MI mice compared with sham-operated mice. However, end-diastolic pressure and dimension and myocardial stiffness of KO+MI were lower than those of the WT+MI mice. Histological examination revealed normal tissue healing, but interstitial fibrosis in the residual myocardium in peri-infarcted areas was significantly less pronounced in KO+MI mice than in WT+MI mice. TN-C may thus accelerate adverse ventricular remodeling, cardiac failure, and fibrosis in the residual myocardium after MI.

extracellular matrix; fibrosis

LEFT VENTRICULAR (LV) REMODELING after myocardial infarction (MI) is a clinically important process, since it may result in dilatation, hypertrophy, and poor prognosis. It is well recognized that ventricular remodeling is accompanied by changes in the structure and composition of the myocardial extracellular matrix (ECM), and the significance of several molecules related to ECM turnover, especially matrix metalloproteinase (MMP)-2 and MMP-9, has received a great deal of attention (reviewed in Ref. 36).

Address for reprint requests and other correspondence: K. Imanaka-Yoshida, Dept. of Pathology and Matrix Biology, Mie Univ. Graduate School of Medicine, 2-174 Edobashi, Tsu, Mie 514-8507, Japan (e-mail: imanaka@doc.medic.mie-u.ac.jp).

Tenascins (TN) are a family of four multimeric ECM glycoproteins, each with distinct features; they are named TN-C, -X, -R, and -W (44). TN-C, which was found to be the first member of the family expressed during embryonic development, as well as in wound healing and cancer invasion in various tissues, may regulate cell behavior and matrix organization during tissue remodeling. In vitro studies suggest that TN-C controls the balance of cell adhesion and deadhesion, as well as cell motility, proliferation, differentiation, and survival (6).

TN-C is not expressed in healthy adult hearts, but is upregulated under many pathological conditions (9, 16, 18, 26, 28, 39), such as acute MI (15, 30, 34, 38, 45), and some cases of dilated cardiomyopathy (39, 43) associated with tissue injury and inflammation (16, 26, 28, 43). After MI, TN-C appears during the acute stage at the interface between infarcts and intact myocardium, where tissue remodeling most actively occurs (15). Our laboratory previously reported that TN-C may weaken the links between cardiomyocytes and connective tissue and accelerate the recruitment of myofibroblasts to injured sites; therefore, it might play an important role in myocardial tissue healing (15, 38).

Although TN-C molecules are deposited in extracellular spaces and regulate local cell behavior, soluble forms are released into the bloodstream. Interestingly, TN-C serum levels are elevated in acute MI patients and so provide a possible predictor of ventricular remodeling and poor prognosis after infarction (34). We and other groups have reported increased serum TN-C in patients who have suffered heart failure, reflecting ventricular remodeling and poor prognosis (10, 12, 25, 40); this suggests an adverse effect on the progression of ventricular remodeling. Conversely, upregulation of TN-C might reflect complementary responses to heart failure, as with the natriuretic peptide system, since various remodeling modulators, such as proinflammatory cytokines, growth factors, angiotensin II, hypoxia, reactive oxygen species, and acidosis, in addition to mechanical stretch, increase synthesis of TN-C by cardiac fibroblasts in vitro (5, 17, 28, 47).

To investigate whether TN-C exacerbates ventricular remodeling, we examined its effects by targeted deletion of TN-C in an experimental model of MI in mice. TN-C knockout (TNKO) mice were independently generated by two different groups and described as showing no distinct morphological phenotypes (8, 33). However, recent detailed studies have shown differences in specific cell behavior and response, particularly in various disease models, such as attenuated fibrotic change in

immune-mediated hepatitis (7), allergic inflammation in bronchial asthma (27) and arthritis (24), reduced neointimal hyperplasia after vascular surgery (48), and delayed repair of articular cartilage injury (31). In the present study, we compared cardiac remodeling in TNKO and wild-type (WT) mice after permanent coronary ligation by echocardiographic and hemodynamic measurements and histological analysis.

MATERIALS AND METHODS

Animals. The investigation was performed in line with the *Guide for the Care and Use of Laboratory Animals* published by the US National Institutes of Health (publication no. 85-23, revised 1996) and was approved by our Institutional Animal Research Committee. The original TNKO mouse (33) was backcrossed with BALB/c inbred mice for more than 10 generations. TN-C-null (−/−) male mice, aged between 8 and 10 wk old, were used in the experiments. WT (+/+) littermates were used as controls.

MI. The MI model involved ligation of the left coronary artery of male TNKO mice (KO+MI group) and sibling WT mice (WT+MI group) under anesthesia, in accordance with the methods described by Michael et al. (23). A sham operation without coronary artery ligation was also performed for both WT (WT+sham) and TNKO (KO+sham) mice.

Survival. For survival analysis of the WT+MI (n = 35) and KO+MI (n = 30) mice, the cages were inspected daily to record the deaths of animals during the 4-wk study period.

Echocardiographic and hemodynamic measurements. Four weeks after ligation, echocardiographic studies were performed, as previously described (11), on surviving WT+MI (n = 16), KO+MI (n = 16), WT+sham (n = 11), and KO+sham (n = 11) mice under light anesthesia with tribromoethanol-amylene hydrate [Avertin; 2.5% (wt/vol), 8 ml/g ip] and spontaneous respiration. After the echocardiographic measurements, LV pressure was measured in accordance with the methods described by Williams et al. (46). Two investigators (M. Ikeuchi and H. Matsusaka.), who were not provided with information about the experimental groups, performed in vivo LV function studies that included echocardiography and LV pressure measurements. Our laboratory's recent validation study demonstrated that intraobserver and interobserver variability with our echocardiographic measurements for LV cavity dimensions and fractional shortening were small, and measurements made in the same animals on separate days were highly reproducible, as previously described (11, 35).

Myocardial stiffness. To determine the myocardial stiffness constant, the σ-ln(1/H) value of the LV regional wall was evaluated with a spherical model of the ventricle to calculate mean wall stress (σ) using the equation $\sigma = PD/4H$, where P is LV pressure, D is LV short-axis diameter, and H is the mean wall thickness of LV anterior and posterior walls (13, 22). The diastolics = ln(1/H) data points from the point of minimal wall stress to the end-diastole point were fitted to a single exponential curve with zero asymptote $\sigma = C \exp [K \ln(1/H)]$, where K is the myocardial stiffness constant.

Tissue preparation. At *day 28*, all surviving mice were killed after echocardiographic and hemodynamic examinations, and their hearts were removed for histological analysis. WT-MI mouse hearts were excised at *days 1*, *2*, *3*, *5*, *7*, and *14* after coronary ligation (n = 3 for each time point). KO-MI mouse hearts at *day 5* (n = 3) were also excised for histological comparison. The entire LV from the apex to the base was cut into three transverse sections, fixed in 4% paraformaldehyde and embedded in paraffin. Sections were cut to a thickness of 3 μm.

Infarct size. Infarct size at *day 28* was analyzed as described by Pfeffer et al. (32). Infarct length was measured along the endocardial and epicardial surfaces in each of the LV sections, and the values from the three sections were summed. Total LV circumference was calculated as the sum of endocardial and epicardial segment lengths from all LV sections. Infarct size (in percent) was calculated as total infarct circumference divided by total LV circumference. The reliability of this measurement was confirmed, as previously described (11).

Image analysis. To detect interstitial collagen fibers, picrosirius red staining was performed using a Scion imaging system, as previously described (28). Collagen volume fraction was measured in six fields of both border zones and remote areas of LVs for each heart in the MI and corresponding sham-operated groups.

Immunohistochemistry. Immunostaining of tissue sections was performed as previously described (15). In brief, after treatment with pepsin for 10 min for antigen retrieval, sections were incubated with anti-TN-C polyclonal rabbit antibody overnight at 4°C and subsequently with peroxidase-conjugated anti-rabbit IgG Fab′ (1:500 MBL, Nagoya, Japan) for 1 h. After washing, diaminobenzidine/H_2O_2 solution was used to demonstrate antibody binding.

RT-PCR. LV myocardial tissues of WT+sham and WT+MI mice on 1, 3, 5, 7 and 14 days after coronary ligation were homogenized in Isogen (NipponGene, Toyama, Japan). Total RNA was isolated, and RT-PCR was performed as previously described (29). The forward and reverse primers for TN-C were 5′-GTTTGGAGACCGCAGAGAAGAA-3′ and 5′-TGTCCCCATATCTGCCCATCA-3′, respectively. The expected size of the PCR fragment was 344 bp. β-Actin was used as an internal control, with forward and reverse primers of 5′-GTGGGGCGCCCCAGGCACCA-3′ and 5′-CTCCTTAATGTCACGCACGATTTC-3′, respectively, and the expected size of the PCR fragment was 571 bp.

Western blot analysis. Protein was extracted from homogenized tissue in Isogen in accordance with the manufacturer's instructions. Samples (10 μg/lane) were subjected to SDS-PAGE with 2–15% gradation polyacrylamide gel, transferred onto Immobilon membranes (Millipore, Bedford, MA), and immunostained with anti-TN-C antibody (1 μg/ml) using the indirect immunoperoxidase method, as previously described (15). Immunoreactivity was detected with the ECL system (Amersham, Arlington Heights, IL).

Statistical analysis. All data are expressed as means ± SE. Survival was analyzed by the Kaplan-Meier method. For between-group analysis, multiple-comparison tests were performed using one-way ANOVA followed by Bonferroni's post hoc test.

RESULTS

Expression of TN-C after MI. In WT-MI mice, the level of TN-C mRNA was upregulated beginning at *day 1* after injury, downregulated at *day 7*, and not detectable at *day 14* (Fig. 1*A*). TN-C protein also became detectable at *day 1*, peaked at *day 5*, then was downregulated until disappearance at *day 14* (Fig. 1*B*). Immunostaining for TN-C (Fig. 1*C*) was observed at the borders between intact myocardial tissues and necrotic areas at *day 1*. Strong staining for TN-C was detected in developing granulation tissue around *days 3–5* and disappeared by *day 28*. No immunoreactivity was detected in remote areas at any stage.

Myocardial repair in TNKO mouse. Myocardial healing associated with granulation tissue formation appeared to proceed normally in KO mice, and there was no obvious difference from WT mice on routine histological analysis (Fig. 2). No immunoreactivity for TN-C was observed in any tissue sections collected from TNKO mice.

Survival. Early operative mortality was comparable between KO and WT mice, and 15/35 (43%) WT+MI and 12/30 (40%) KO+MI mice died within 24 h after ligation. Between *weeks 1* and *4* after surgery, four WT+MI (11.4%) and one KO+MI (3%) mice died of heart failure. One KO+MI mouse died of heart rupture at *day 8*, while no rupture was observed in the WT+MI group. At *day 28*, no significant difference in the

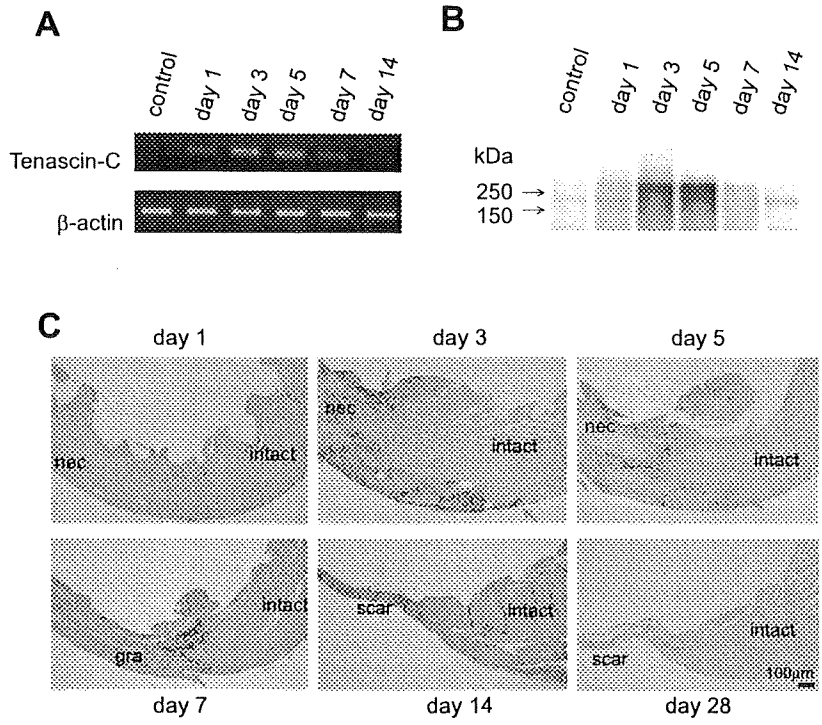

Fig. 1. *A*: RT-PCR analysis of the expression of tenascin (TN)-C in myocardium of normal mouse (control) at *days 1*, *3*, *5*, *7*, and *14* after coronary ligation. *B*: Western blot analysis of myocardium of normal mouse (control) at *days 1*, *3*, *5*, *7*, and *14* after coronary ligation. Two isoforms at ~210 and 280 kDa became detectable at *day 1*, peaked at *day 5*, but had disappeared at *day 7*. *C*: immunostaining for TN-C in mouse myocardium at *days 1*, *3*, *5*, *7*, *14*, and *28* after coronary ligation. Note that TN-C deposition (orange arrows) was detectable at *day 1* in the border zones between intact myocardial tissues and infarcted areas, peaked at *days 3–5*, and disappeared by *day 28*. intact, Intact area; nec, necrotic area: gra, granulation tissue; scar, scar tissue.

survival rate was found between the WT and KO groups (49 vs. 57%; Fig. 3*A*).

Mice at day 28 after coronary ligation. See Table 1. The surviving mice at *day 28* were killed after echocardiographic and hemodynamic measurements. WT+MI lung-to-body weight ratios and right ventricle (RV)-to-body weight ratios of WT+MI were significantly increased compared with those of the WT+sham mice. No significant difference in lung-to-body weight ratios and RV-to-body weight ratios was found between the KO+sham and KO+MI group. RV-to-body weight ratios of KO+MI were significantly lower than in the WT+MI mice.

Infarct size. Infarct sizes determined by morphometric analysis 28 days after ligation were comparable (59 ± 9.3 vs. 55.5 ± 7.5%, P = not significant) between the WT+MI (n = 6) and KO+MI (n = 6) mice (Fig. 3*B*).

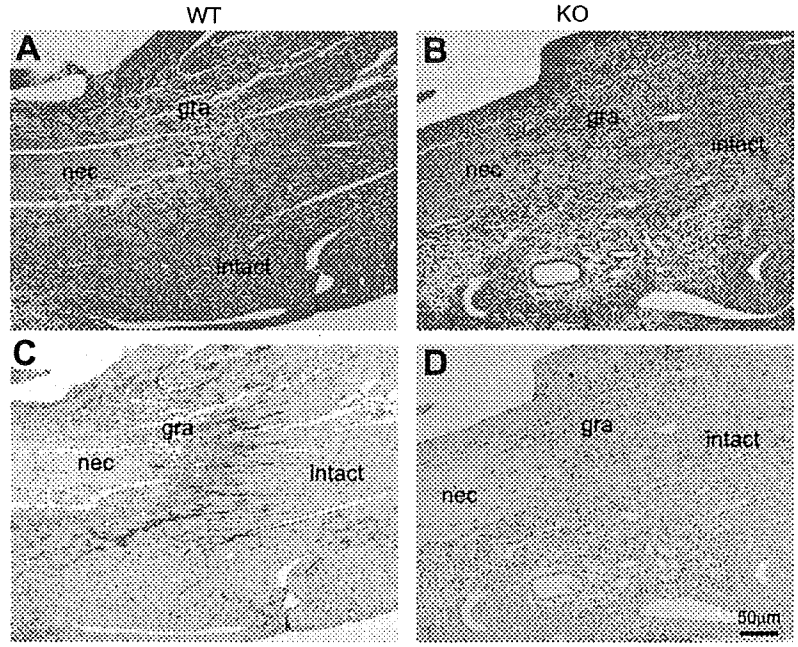

Fig. 2. Representative photomicrographs of border zone myocardium obtained from wild-type (WT) + myocardial infarction (MI) mice (*A* and *C*) and TN-C knockout (KO) + MI mice (*B* and *D*) 5 days after coronary ligation, stained with hematoxylin and eosin (*A* and *B*) or immunostained with anti-TN-C antibody (*B* and *D*). Positive staining of TN-C is evident at peri-infarcted areas of WT mice, whereas no signals are apparent in the KO mice. No obvious histological differences are visible between WT and KO.

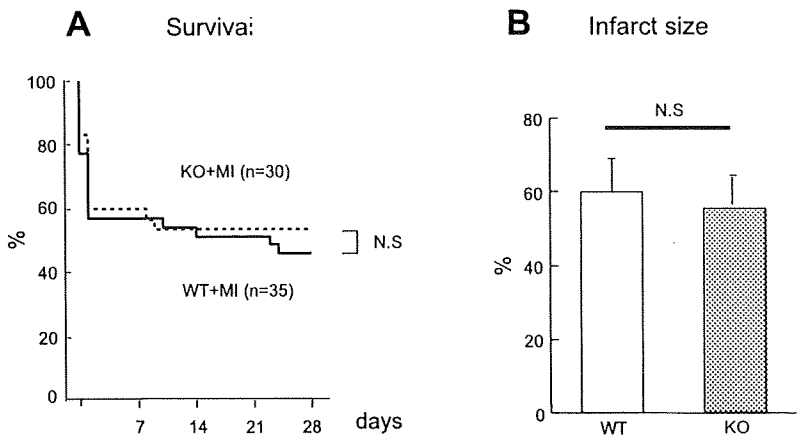

Fig. 3. *A*: survival after MI of WT+MI and KO+MI mice. Animals were observed for up to 28 days after surgery. *B*: morphometrically determined infarct size in WT+MI and KO+MI mice at *day 28*. NS, not significant.

Cardiac function, stiffness, and remodeling. See Table 2. There were no significant differences in LV size and function between sham-operated KO and WT mice. In WT+MI mice, LV end-diastolic diameter increased significantly, accompanied by a reduced ejection fraction compared with those in WT+sham mice. Myocardial stiffness and LV end-diastolic pressure also increased in WT+MI mice. In KO+MI mice, LV end-diastolic diameter and LV end-diastolic pressure showed similar significant increases compared with those of KO+sham mice ($P < 0.01$ and $P < 0.05$, respectively). However, end-diastolic pressure and dimension and myocardial stiffness were lower than in the WT+MI mice, suggesting that TN-C plays an important role in LV remodeling and stiffness.

Fibrosis. Quantitative analysis of the percentage of interstitial collagen volume in the residual myocardium at border zones revealed a significant increase in the WT+MI mice compared with the WT+sham mice (11.3 ± 1.0 vs. 0.9 ± 0.4%, $P < 0.01$). In the KO+MI case, percentage of interstitial collagen volume was also greater than that in KO+sham mice (7.3 ± 2.3 vs. 1.2 ± 0.4%, $P < 0.01$), but was significantly reduced compared with that in WT+MI mice ($P < 0.01$). In remote zones, no significant differences in percentage of fibrotic area were found between either WT+sham and KO+sham mice (0.8 ± 0.3 vs. 1.1 ± 0.4%, P = not significant) or WT+MI and KO+MI mice (2.3 ± 1.4 vs. 2.0 ± 0.9%, P = not significant) (Fig. 4).

DISCUSSION

The present study clearly demonstrated that TN-C is involved in the progression of adverse ventricular remodeling after MI. Targeted deletion improved cardiac function and myocardial stiffness, in association with the reduction in interstitial fibrosis in the border zone myocardium, where TN-C expression was localized, while it did not appear to change in remote areas of the residual myocardium.

In the mouse MI model, both TN-C mRNA and TN-C protein became detectable at *day 1* after coronary ligation, peaked at *day 5*, then were downregulated and disappeared by *day 28*, when infarcted areas were replaced by scar tissue. During the healing process, TN-C was only localized in the border zones and was not detected in the intact myocardium. This spatiotemporal expression pattern is comparable with previous results observed in an experimental rat model (15) and a human myocardial sample obtained at autopsy (45).

It has been proposed that TN-C plays an important role in tissue repair in various organs based on its specific expression that is closely associated with injury and inflammation. A number of studies have demonstrated that TN-C promotes proliferation and migration of parenchymal epithelial cells (37, 49) and angiogenesis (1). Furthermore, we previously reported that TN-C accelerates migration and differentiation of myofibroblasts (38), which play an important role in wound healing by synthesizing collagens and exerting strong contractive forces to promote wound healing. These functions expedite tissue healing, may protect against cardiac rupture, and prevent ventricular dilatation after MI.

On the other hand, TN-C may also promote adverse ventricular remodeling. For example, TN-C weakens the adhesion of cardiomyocytes to connective tissue (15) and upregulates expression and activity of MMP-2 and -9 (14, 20, 27, 42). Furthermore, there is a growing body of evidence suggesting that TN-C enhances inflammatory responses (24) with activa-

Table 1. *Organ weights of mice at day 28 after coronary ligation*

	WT+Sham	KO+Sham	WT+MI	KO+MI
n	11	11	16	16
Organ weights				
Body weight, g	23.3 ± 0.5	24.8 ± 0.9	25.5 ± 0.4*	25.7 ± 0.5
LV weight/body weight, mg/g	3.12 ± 0.01	3.06 ± 0.15	3.28 ± 0.13	3.13 ± 0.14
RV weight/body weight, mg/g	0.80 ± 0.01	0.87 ± 0.12	1.19 ± 0.11*	0.95 ± 0.11*‡
Lung weight/body weight, mg/g	5.53 ± 0.17	5.44 ± 0.65	7.47 ± 0.65*	6.50 ± 0.19†
Pleural effusion, %			44	19

Values are means ± SE; *n*, no. of mice. WT, wild type; KO, knockout; MI, myocardial infarction; LV, left ventricular; RV, right ventricular. *$P < 0.05$ and †$P < 0.01$ vs. WT+sham. ‡$P < 0.05$ vs. WT+MI.

Table 2. *Echocardiographic and hemodynamic data at day 28 after coronary ligation*

	WT+Sham	KO+Sham	WT+MI	KO+MI
n	11	11	16	16
Echocardiography				
Heart rate, beats/min	459 ± 9	458 ± 5	469 ± 5	461 ± 6
LVEDD, mm	3.5 ± 0.1	3.5 ± 0.1	5.6 ± 0.1†	5.2 ± 0.1†‡
Ejection fraction, %	75.5 ± 0.8	75.2 ± 0.9	35.6 ± 1.2†	41.2 ± 1.3†‡
Fractional shortening, %	37.5 ± 0.7	37.2 ± 0.7	13.7 ± 0.5†	16.3 ± 0.6†‡
Infarct wall thickness, mm	—	—	0.33 ± 0.02	0.31 ± 0.02
Noninfarct wall thickness, mm	0.74 ± 0.01	0.75 ± 0.03	0.87 ± 0.03†	0.83 ± 0.03†
Hemodynamics				
Heart rate, beats/min	449 ± 8	444 ± 7	438 ± 5	441 ± 8
Mean blood pressure, mmHg	86 ± 3	86 ± 2	84 ± 2	85 ± 2
LVEDP, mmHg	2.0 ± 0.4	3.0 ± 0.8	15.1 ± 2.0†	9.0 ± 1.3†‡
LV dP/dt_{max}, mmHg/s	10,725 ± 642	9,452 ± 422	7,305 ± 461†	8,059 ± 381*
LV dP/dt_{min}, mmHg/s	−9,509 ± 543	−8,368 ± 472	−4,755 ± 327†	−5,478 ± 259†
Myocardial stiffness	2.7 ± 0.3	3.6 ± 0.5	6.7 ± 0.5†	5.1 ± 0.4†‡

Values are means ± SE; *n*, no. of mice. LVEDD, LV end-diastolic diameter; LVEDP, LV end-diastolic pressure; LV dP/dt_{max}, maximal first derivative of left ventricular pressure; LV dP/dt_{min}, minimal first derivative of left ventricular pressure. *$P < 0.05$ and †$P < 0.01$ vs. WT+sham. ‡$P < 0.01$ vs. WT+MI.

tion of NF-κB (27) and cytokine upregulation (7). Although these functions are useful for clearing damaged tissue and releasing residual cardiomyocytes from connective tissue for rearrangement, they might cause progressive degradation of ECMs and slippage of myocytes within the LV wall.

Moreover, a system that compensates for a lack of TN-C apparently exists (8, 18, 21, 33). The recruitment of myofibroblasts to injured sites of myocardium is delayed in TNKO mice, but approaches that of WT mice by *day 3* after injury (38); however, the compensatory mechanism has not been identified. Therefore, it is difficult to theoretically determine whether TN-C is harmful or beneficial overall for tissue reconstruction after MI.

In the present study, during the acute stage, tissue healing in TNKO mice seemed to proceed normally with no difference in

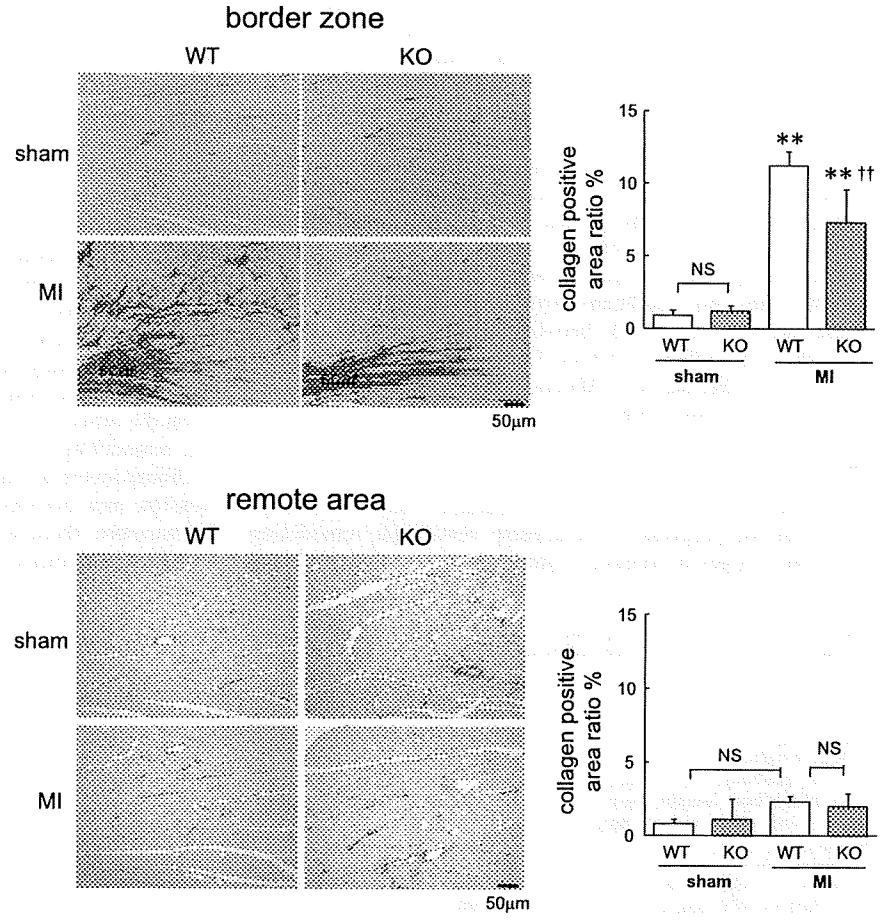

Fig. 4. Quantitative analysis of percentage of interstitial collagen volume in residual myocardium of border zones and remote areas at *day 28*. **$P < 0.01$ vs. WT+sham. ††$P < 0.01$ vs. WT+MI.

survival rate compared with that in WT mice. However, ventricular remodeling was significantly reduced in the TNKO mice, and cardiac function was improved at *day 28* after coronary ligation. It seems that TN-C plays critical roles in the modulation of responses to myocardial injury and exerts harmful effects on the heart at later stages. The results correspond to our laboratory's recent clinical finding that patients with high serum levels of TN-C in the acute stage within 1 wk after infarction have a greater incidence of ventricular remodeling 6 mo later and a worse long-term prognosis (34).

Histologically, interstitial fibrosis of residual myocardium at *day 28* in TNKO animals was markedly reduced compared with that in the WT mice in peri-infarct areas, where TN-C is normally deposited during the acute stage. Thus it is suggested that the deletion of TN-C may alleviate the progression of fibrosis, which could contribute to improvement of myocardial stiffness.

It has been proposed that TN-C promotes fibrosis because of its upregulated expression in various fibrogenic processes (2, 6, 19, 28). Direct support for this is the finding that locally applied TN-C accelerates the recruitment of myofibroblasts and collagen fiber formation in aneurysmal cavities in a rat model (41). Furthermore, deficiency of TN-C attenuated the expression of collagen I and III in an immune-mediated chronic hepatitis model (7) and deposition of proteoglycan in neointima after aortotomy in mice (48).

Although multiple molecular pathways are involved in the progression of ventricular remodeling and fibrosis, transforming growth factor (TGF)-β/Smad3 signaling may be a cascade of major importance (reviewed in Ref. 3). Loss of Smad3 results in a very similar phenotype to that evident in our TNKO mice, demonstrating reduced interstitial fibrosis and attenuation of remodeling associated with downregulation of TN-C (4). Since TGF-β is a strong inducer of TN-C in cardiac fibroblasts (26), TN-C may be a key molecule in the cascade of TGF-β/Smad3 signaling in ventricular remodeling.

In conclusion, TN-C may aggravate unfavorable responses during myocardial repair and could, therefore, be a target molecule for prevention of adverse ventricular remodeling after MI.

ACKNOWLEDGMENTS

The authors express deep gratitude to Dr. Shinobu Arai for helpful advice on the statistical analysis and to Akiyo Sekimoto, Mari Hara, and Miyuki Namikata for technical assistance.

GRANTS

This study was supported in part by a Grant-in-aid for scientific research (no. 21590927) from the Ministry of Education, Culture, Sports, Science and Technology of Japan (to K. Imanaka-Yoshida), a research grant for intractable diseases from the Ministry of Health, Labor and Welfare of Japan (to K. Imanaka-Yoshida and M. Hiroe), and a grant from the Japan Foundation for the Promotion of the International Medical Center of Japan (to M. Hiroe and K. Imanaka-Yoshida).

DISCLOSURES

No conflicts of interest are declared by the author(s).

REFERENCES

1. **Ballard VLT, Sharma A, Duignan I, Holm JM, Chin A, Choi R, Hajjar KA, Wong SC, Edelberg JM.** Vascular tenascin-c regulates cardiac endothelial phenotype and neovascularization. *FASEB J* 20: 717–719, 2006.
2. **Brellier F, Tucker RP, Chiquet-Ehrismann R.** Tenascins and their implications in diseases and tissue mechanics. *Scand J Med Sci Sports* 19: 511–519, 2009.
3. **Bujak M, Frangogiannis NG.** The role of TGF-beta signaling in myocardial infarction and cardiac remodeling. *Cardiovasc Res* 74: 184–195, 2007.
4. **Bujak M, Ren G, Kweon HJ, Dobaczewski M, Reddy A, Taffet G, Wang XF, Frangogiannis NG.** Essential role of smad3 in infarct healing and in the pathogenesis of cardiac remodeling. *Circulation* 116: 2127–2138, 2007.
5. **Chiquet M, Sarasa-Renedo A, Tunc-Civelek V.** Induction of tenascin-C by cyclic tensile strain versus growth factors: distinct contributions by Rho/ROCK and MAPK signaling pathways. *Biochim Biophys Acta* 1693: 193–204, 2004.
6. **Chiquet-Ehrismann R, Chiquet M.** Tenascins: regulation and putative functions during pathological stress. *J Pathol* 200: 488–499, 2003.
7. **El-Karef A, Yoshida T, Gabazza EC, Nishioka T, Inada H, Sakakura T, Imanaka-Yoshida K.** Deficiency of tenascin-C attenuates liver fibrosis in immune-mediated chronic hepatitis in mice. *J Pathol* 211: 86–94, 2007.
8. **Forsberg E, Hirsch E, Frohlich L, Meyer M, Ekblom P, Aszodi A, Werner S, Fassler R.** Skin wounds and severed nerves heal normally in mice lacking tenascin-C. *Proc Natl Acad Sci U S A* 93: 6594–6599, 1996.
9. **Frangogiannis NG, Shimoni S, Chang SM, Ren G, Dewald O, Gersch C, Shan K, Aggeli C, Reardon M, Letsou GV, Espada R, Ramchandani M, Entman ML, Zoghbi WA.** Active interstitial remodeling: an important process in the hibernating human myocardium. *J Am Coll Cardiol* 39: 1468–1474, 2002.
10. **Fujimoto N, Onishi K, Sato A, Terasaki F, Tsukada B, Nozato T, Yamada T, Imanaka-Yoshida K, Yoshida T, Ito M, Hiroe M.** Incremental prognostic values of serum tenascin-C levels with blood b-type natriuretic peptide testing at discharge in patients with dilated cardiomyopathy and decompensated heart failure. *J Card Fail* 15: 898–905, 2009.
11. **Hayashidani S, Tsutsui H, Ikeuchi M, Shiomi T, Matsusaka H, Kubota T, Imanaka-Yoshida K, Itoh T, Takeshita A.** Targeted deletion of MMP-2 attenuates early LV rupture and late remodeling after experimental myocardial infarction. *Am J Physiol Heart Circ Physiol* 285: H1229–H1235, 2003.
12. **Hessel MH, Bleeker GB, Bax JJ, Henneman MM, den Adel B, Klok M, Schalij MJ, Atsma DE, van der Laarse A.** Reverse ventricular remodelling after cardiac resynchronization therapy is associated with a reduction in serum tenascin-c and plasma matrix metalloproteinase-9 levels. *Eur J Heart Fail* 9: 1058–1063, 2007.
13. **Higashita R, Sugawara M, Kondoh Y, Kawai Y, Mitsui K, Ohki S, Tange S, Ichikawa S, Suma K.** Changes in diastolic regional stiffness of the left ventricle before and after coronary artery bypass grafting. *Heart Vessels* 11: 145–151, 1996.
14. **Ilunga K, Nishiura R, Inada H, El-Karef A, Imanaka-Yoshida K, Sakakura T, Yoshida T.** Co-stimulation of human breast cancer cells with transforming growth factor-beta and tenascin-C enhances matrix metalloproteinase-9 expression and cancer cell invasion. *Int J Exp Pathol* 85: 373–379, 2004.
15. **Imanaka-Yoshida K, Hiroe M, Nishikawa T, Ishiyama S, Shimojo T, Ohta Y, Sakakura T, Yoshida T.** Tenascin-C modulates adhesion of cardiomyocytes to extracellular matrix during tissue remodeling after myocardial infarction. *Lab Invest* 81: 1015–1024, 2001.
16. **Imanaka-Yoshida K, Hiroe M, Yasutomi Y, Toyozaki T, Tsuchiya T, Noda N, Maki T, Nishikawa T, Sakakura T, Yoshida T.** Tenascin-C is a useful marker for disease activity in myocarditis. *J Pathol* 197: 388–394, 2002.
17. **Imanaka-Yoshida K, Hiroe M, Yoshida T.** Interaction between cell and extracellular matrix in heart disease: multiple roles of tenascin-C in tissue remodeling. *Histol Histopathol* 19: 517–525, 2004.
18. **Imanaka-Yoshida K, Matsumoto K, Hara M, Sakakura T, Yoshida T.** The dynamic expression of tenascin-C and tenascin-X during early heart development in the mouse. *Differentiation* 71: 291–298, 2003.
19. **Jones PL, Jones FS.** Tenascin-C in development and disease: gene regulation and cell function. *Matrix Biol* 19: 581–596, 2000.
20. **Kalembeyi I, Inada H, Nishiura R, Imanaka-Yoshida K, Sakakura T, Yoshida T.** Tenascin-C up-regulates matrix metalloproteinase-9 in breast cancer cells: direct and synergistic effects with transforming growth factor beta 1. *Int J Cancer* 105: 53–60, 2003.
21. **Mackie EJ, Tucker RP.** The tenascin-C knockout revisited. *J Cell Sci* 112: 3847–3853, 1999.

22. **Masuyama T, Yamamoto K, Sakata Y, Doi R, Nishikawa N, Kondo H, Ono K, Kuzuya T, Sugawara M, Hori M.** Evolving changes in doppler mitral flow velocity pattern in rats with hypertensive hypertrophy. *J Am Coll Cardiol* 36: 2333–2338, 2000.
23. **Michael LH, Entman ML, Hartley CJ, Youker KA, Zhu J, Hall SR, Hawkins HK, Berens K, Ballantyne CM.** Myocardial ischemia and reperfusion: a murine model. *Am J Physiol Heart Circ Physiol* 269: H2147–H2154, 1995.
24. **Midwood K, Sacre S, Piccinini AM, Inglis J, Trebaul A, Chan E, Drexler S, Sofat N, Kashiwagi M, Orend G, Brennan F, Foxwell B.** Tenascin-C is an endogenous activator of toll-like receptor 4 that is essential for maintaining inflammation in arthritic joint disease. *Nat Med* 15: 774–780, 2009.
25. **Milting H, Ellinghaus P, Seewald M, Cakar H, Bohms B, Kassner A, Korfer R, Klein M, Krahn T, Kruska L, El Banayosy A, Kramer F.** Plasma biomarkers of myocardial fibrosis and remodeling in terminal heart failure patients supported by mechanical circulatory support devices. *J Heart Lung Transplant* 27: 589–596, 2008.
26. **Morimoto S, Imanaka-Yoshida K, Hiramitsu S, Kato S, Ohtsuki M, Uemura A, Kato Y, Nishikawa T, Toyozaki T, Hishida H, Yoshida T, Hiroe M.** Diagnostic utility of tenascin-C for evaluation of the activity of human acute myocarditis. *J Pathol* 205: 460–467, 2005.
27. **Nakahara H, Gabazza EC, Fujimoto H, Nishii Y, D'Alessandro-Gabazza CN, Bruno NE, Takagi T, Hayashi T, Maruyama J, Maruyama K, Imanaka-Yoshida K, Suzuki K, Yoshida T, Adachi Y, Taguchi O.** Deficiency of tenascin C attenuates allergen-induced bronchial asthma in the mouse. *Eur J Immunol* 36: 3334–3345, 2006.
28. **Nishioka T, Suzuki M, Onishi K, Takakura N, Inada H, Yoshida T, Hiroe M, Imanaka-Yoshida K.** Eplerenone attenuates myocardial fibrosis in the angiotensin II-induced hypertensive mouse: involvement of tenascin-C induced by aldosterone-mediated inflammation. *J Cardiovasc Pharmacol* 49: 261–268, 2007.
29. **Noda N, Minoura H, Nishiura R, Toyoda N, Imanaka-Yoshida K, Sakakura T, Yoshida T.** Expression of tenascin-C in stromal cells of the murine uterus during early pregnancy: induction by interleukin-1 alpha, prostaglandin E(2), and prostaglandin F(2 alpha). *Biol Reprod* 63: 1713–1720, 2000.
30. **Odaka K, Uehara T, Arano Y, Adachi S, Tadokoro H, Yoshida K, Hasegawa H, Imanaka-Yoshida K, Yoshida T, Hiroe M, Irie T, Tanada S, Komuro I.** Noninvasive detection of cardiac repair after acute myocardial infarction in rats by 111 in fab fragment of monoclonal antibody specific for tenascin-C. *Int Heart J* 49: 481–492, 2008.
31. **Okamura N, Hasegawa M, Nakoshi Y, Iino T, Sudo A, Imanaka-Yoshida K, Yoshida T, Uchida A.** Deficiency of tenascin-C delays articular cartilage repair in mice. *Osteoarthritis Cartilage.* In press.
32. **Pfeffer MA, Pfeffer JM, Fishbein MC, Fletcher PJ, Spadaro J, Kloner RA, Braunwald E.** Myocardial infarct size and ventricular function in rats. *Circ Res* 44: 503–512, 1979.
33. **Saga Y, Yagi T, Ikawa Y, Sakakura T, Aizawa S.** Mice develop normally without tenascin. *Genes Dev* 6: 1821–1831, 1992.
34. **Sato A, Aonuma K, Imanaka-Yoshida K, Yoshida T, Isobe M, Kawase D, Kinoshita N, Yazaki Y, Hiroe M.** Serum tenascin-C might be a novel predictor of left ventricular remodeling and prognosis after acute myocardial infarction. *J Am Coll Cardiol* 47: 2319–2325, 2006.
35. **Shiomi T, Tsutsui H, Hayashidani S, Suematsu N, Ikeuchi M, Wen J, Ishibashi M, Kubota T, Egashira K, Takeshita A.** Pioglitazone, a peroxisome proliferator-activated receptor-γ agonist, attenuates left ventricular remodeling and failure after experimental myocardial infarction. *Circulation* 106: 3126–3132, 2002.
36. **Spinale FG.** Myocardial matrix remodeling and the matrix metalloproteinases: influence on cardiac form and function. *Physiol Rev* 87: 1285–1342, 2007.
37. **Stepp MA, Zhu L.** Up-regulation of α9 integrin and tenascin during epithelial regeneration after debridement in the cornea. *J Histochem Cytochem* 45: 189–202, 1997.
38. **Tamaoki M, Imanaka-Yoshida K, Yokoyama K, Nishioka T, Inada H, Hiroe M, Sakakura T, Yoshida T.** Tenascin-C regulates recruitment of myofibroblasts during tissue repair after myocardial injury. *Am J Pathol* 167: 71–80, 2005.
39. **Tamura A, Kusachi S, Nogami K, Yamanishi A, Kajikawa Y, Hirohata S, Tsuji T.** Tenascin expression in endomyocardial biopsy specimens in patients with dilated cardiomyopathy: distribution along margin of fibrotic lesions. *Heart* 75: 291–294, 1996.
40. **Terasaki F, Okamoto H, Onishi K, Sato A, Shimomura H, Tsukada B, Imanaka-Yoshida K, Hiroe M, Yoshida T, Kitaura Y, Kitabatake A.** Higher serum tenascin-C levels reflect the severity of heart failure, left ventricular dysfunction and remodeling in patients with dilated cardiomyopathy. *Circ J* 71: 327–330, 2007.
41. **Toma N, Imanaka-Yoshida K, Takeuchi T, Matsushima S, Iwata H, Yoshida T, Taki W.** Tenascin-C coated on platinum coils for acceleration of organization of cavities and reduction of lumen size in a rat aneurysm model. *J Neurosurg* 103: 681–686, 2005.
42. **Tremble P, Chiquet-Ehrismann R, Werb Z.** The extracellular matrix ligands fibronectin and tenascin collaborate in regulating collagenase gene expression in fibroblasts. *Mol Biol Cell* 5: 439–453, 1994.
43. **Tsukada B, Terasaki F, Shimomura H, Otsuka K, Otsuka K, Katashima T, Fujita S, Imanaka-Yoshida K, Yoshida T, Hiroe M, Kitaura Y.** High prevalence of chronic myocarditis in dilated cardiomyopathy referred for left ventriculoplasty: expression of tenascin-C as a possible marker for inflammation. *Hum Pathol* 40: 1015–1022, 2009.
44. **Tucker RP, Chiquet-Ehrismann R.** The regulation of tenascin expression by tissue microenvironments. *Biochim Biophys Acta* 1793: 888–892, 2009.
45. **Willems IE, Arends JW, Daemen MJ.** Tenascin and fibronectin expression in healing human myocardial scars. *J Pathol* 179: 321–325, 1996.
46. **Williams RV, Lorenz JN, Witt SA, Hellard DT, Khoury PR, Kimball TR.** End-systolic stress-velocity and pressure-dimension relationships by transthoracic echocardiography in mice. *Am J Physiol Heart Circ Physiol* 274: H1828–H1835, 1998.
47. **Yamamoto K, Dang QN, Kennedy SP, Osathanondh R, Kelly RA, Lee RT.** Induction of tenascin-C in cardiac myocytes by mechanical deformation. Role of reactive oxygen species. *J Biol Chem* 274: 21840–21846, 1999.
48. **Yamamoto K, Onoda K, Sawada Y, Fujinaga K, Imanaka-Yoshida K, Shimpo H, Yoshida T, Yada I.** Tenascin-C is an essential factor for neointimal hyperplasia after aortotomy in mice. *Cardiovasc Res* 65: 737–742, 2005.
49. **Yoshimura E, Majima A, Sakakura Y, Sakakura T, Yoshida T.** Expression of tenascin-C and the integrin alpha 9 subunit in regeneration of rat nasal mucosa after chemical injury: involvement in migration and proliferation of epithelial cells. *Histochem Cell Biol* 111: 259–264, 1999.

The IκB Kinase β/Nuclear Factor κB Signaling Pathway Protects the Heart From Hemodynamic Stress Mediated by the Regulation of Manganese Superoxide Dismutase Expression

Shungo Hikoso, Osamu Yamaguchi, Yuko Nakano, Toshihiro Takeda, Shigemiki Omiya, Isamu Mizote, Manabu Taneike, Takafumi Oka, Takahito Tamai, Jota Oyabu, Yoshihiro Uno, Yasushi Matsumura, Kazuhiko Nishida, Keiichiro Suzuki, Mikihiko Kogo, Masatsugu Hori, Kinya Otsu

Abstract—Cardiomyocyte death plays an important role in the pathogenesis of heart failure. The nuclear factor (NF)-κB signaling pathway regulates cell death, however, the effect of NF-κB pathway on cell death can vary in different cells or stimuli. The purpose of the present study was to clarify the in vivo role of the NF-κB pathway in response to pressure overload. First, we subjected C57Bl6/J mice to pressure overload by means of transverse aortic constriction (TAC) and examined the activity of the NF-κB pathway in response to pressure overload. IκB kinase (IKK) and NF-κB were activated after TAC. Then, we investigated the role of the activation using cardiac-specific IKKβ-deficient mice (CKO). CKO displayed normal global cardiac structure and function compared with control littermates. We subjected CKO and control mice to pressure overload. One week after TAC, CKO showed cardiac dilation, dysfunction, and lung congestion, which are characteristics of heart failure. The number of apoptotic cells in the hearts of CKO mice increased significantly after TAC. The levels of manganese superoxide dismutase mRNA and protein expression in CKO after TAC were significantly attenuated compared with control mice. The levels of oxidative stress and c-Jun N-terminal kinase (JNK) activation in CKO after TAC were significantly greater than those in control mice. Isoproterenol-induced cell death of isolated adult CKO cardiomyocytes was inhibited by treatment with either a manganese superoxide dismutase mimetic or a JNK inhibitor. Thus, the IKKβ/NF-κB signaling pathway plays a protective role in cardiomyocytes because of the attenuation of oxidative stress and JNK activation in a setting of acute pressure overload. (***Circ Res.* 2009; 105:70-79.**)

Key Words: heart failure ■ apoptosis ■ NF-κB

Cardiac remodeling is generally accepted as a determinant of the clinical course of heart failure. Cardiomyocyte apoptotic death plays an important role in the progression of cardiac remodeling.[1–4] The loss of cardiomyocytes caused by apoptosis is predicted to reduce contractility and promote slippage of muscle bundles, wall thinning, and dilatation, which are commonly observed during heart failure. Neurohumoral factors and cytokines that are induced by mechanical stress on cardiomyocytes activate various intracellular signaling pathways, which regulate apoptotic cell death.

The nuclear factor (NF)-κB transcription factors (p50, p52, RelA, c-Rel, and RelB) play important roles in many physiological and pathological conditions. These transcriptional factors are kept inactive in the cytoplasm by binding of inhibitory proteins, the IκB (inhibitor of NF-κB) family. On stimulation, IκBs are phosphorylated at serine residues, leading to their ubiquitination and degradation by the 26S proteasome. The freed NF-κB components dimerize and translocate to nucleus, where they bind to specific sequences in either the promoter or enhancer regions of target genes.[5] Activation process is dependent on phosphorylation of IκB proteins, which is mediated by the IKK complex. The IKK complex is composed of 2 catalytic subunits (IKKα and IKKβ) and a regulatory subunit (IKKγ or NEMO [NF-κB essential modulator]). In the canonical NF-κB signaling pathway, IKKβ is both necessary and sufficient for phosphorylation of IκBα and IκBβ.[5]

We previously reported that NF-κB is involved in the mechanism of G protein–coupled receptor agonist– or tumor necrosis factor (TNF)-α–induced cardiomyocyte hypertrophy

Original received December 25, 2008; revision received April 28, 2009; accepted May 20, 2009.

From the Departments of Cardiovascular Medicine (S.H., O.Y., T. Takeda, S.O., I.M., M.T., T.O., T. Tamai, J.O., K.N., M.H., K.O.) and Medical Information Science (Y.M.), Graduate School of Medicine; First Department of Oral and Maxillofacial Surgery (Y.N., M.K.), Graduate School of Dentistry; Supply Center of Inbred Animals (Y.U.), Osaka University, Suita; and Department of Biochemistry (K.S.), Hyogo College of Medicine, Nishinomiya, Japan.

Correspondence to Kinya Otsu, MD, PhD, Department of Cardiovascular Medicine, Osaka University Graduate School of Medicine, 2-2 Yamadaoka, Suita, Osaka 565-0871, Japan. E-mail kotsu@medone.med.osaka-u.ac.jp

Circulation Research is available at http://circres.ahajournals.org DOI: 10.1161/CIRCRESAHA.108.193318

in cultured rat neonatal cardiomyocytes.[6,7] The in vivo role of the NF-κB signaling pathway in the heart has been investigated using mice lacking p50. Ablation of p50 improved both cardiac function and survival after myocardial infarction[8,9] and in TNF-α–induced cardiomyopathy.[10] In contrast, reovirus-induced apoptosis was significantly enhanced in the hearts of p50-deficient mice.[11] Thus, the in vivo role of the NF-κB pathway in the pathogenesis of cardiac remodeling remains controversial. Because IKKβ is both necessary and sufficient for phosphorylation of IκBs in the canonical NF-κB signaling pathway, cardiomyocyte-specific knockdown of IKKβ enables investigation of the precise role of NF-κB in cardiomyocytes. The purpose of the present study was to determine whether the IKKβ/NF-κB pathway plays a protective or harmful role in the response of cardiomyocytes to hemodynamic stress, using cardiac-specific IKKβ-deficient mice.

Materials and Methods

Generation of Cardiac-Specific IKKβ-Deficient Mice

We mated *Ikbkβ*$^{flox/flox}$ mice[12] with knock-in mice expressing *Cre* recombinase under control of the myosin light chain 2V promoter (*MLC2V-Cre* mice)[13] to generate *Ikbkβ*$^{flox/flox}$;*MLC2V-Cre*$^{+}$ mice, which harbored the cardiac-specific IKKβ knockout.

This study was carried out under the supervision of the Animal Research Committee of Osaka University and in accordance with the Guidelines for Animal Experiments of Osaka University and the Japanese Animal Protection and Management Law (No. 25).

Transverse Aortic Constriction, Echocardiography, and Hemodynamic Analysis

We performed transverse aortic constriction (TAC), murine transthoracic echocardiography, and hemodynamic measurements.[2] Noninvasive measurements of blood pressure were carried out on mice anesthetized with 2.5% avertin using a BP Monitor for Rats and Mice Model MK-2000 (Muromachi Kikai, Tokyo, Japan) according to the instructions of the manufacturer.

Histological Analysis and Evaluation of Apoptosis

Hematoxylin/eosin or Azan–Mallory staining was performed on paraffin-embedded sections. The cross-sectional areas of cardiomyocytes were determined as previously described.[2] To detect apoptotic cells, triple staining with terminal deoxynucleotidyl transferase–mediated dUTP nick-end labeling (TUNEL), propidium iodide, and anti–α-sarcomeric actin antibody (Sigma) and immunohistochemical staining for activated caspase 3 using anti–activated caspase 3 antibody (Abcam Inc) were performed using paraffin-embedded sections.[14] To detect nuclear accumulation of the NF-κB subunit, we performed immunohistochemical staining for p65 on paraffin-embedded sections with anti-p65 antibody (Santa Cruz Biotechnology).

Western Blot Analysis

Protein homogenates were subjected to Western blot analysis using antibodies against IKKα (IMGENEX), IKKβ (Abcam), NEMO and total c-Jun N-terminal kinase (JNK) (Santa Cruz Biotechnology), phospho-JNK (Cell Signaling Technology), and manganese superoxide dismutase (MnSOD).[15] Signals of the scanned autoradiographs were quantified by densitometric measurements with the Scion Image software (version 4.02; Scion corp.).

Preparation of Nuclear Extract and the Electrophoretic Mobility Shift Assay

Electrophoretic mobility-shift assay (EMSA) was performed as previously described.[7]

Total RNA Extraction, RNA Dot Blot Analysis, and Quantitative Real-Time RT-PCR

Isolation of total RNA and quantitative assessment of mRNA expression by dot blot analysis or quantitative RT-PCR were performed.[2] PCR primers and probes for TNF-α and interleukin (IL)-2 has been previously described.[2] Primers and probes for other targets were obtained from Applied Biosystems. RT-PCR standard curves were constructed using the corresponding cDNA. All data were normalized to GAPDH content and are expressed as fold increase relative to expression in a sham-operated control littermate mouse.

IKK Assay

We immunoprecipitated the IKK complex from extracts containing 0.8 mg protein with an anti-NEMO antibody (Santa Cruz Biotechnology). We measured kinase activity using recombinant human IκBα (Cell Science) as the substrate.[17]

Isolation and Characterization of Adult Mouse Ventricular Myocytes

Mouse adult cardiomyocytes[18] were treated with 50 μmol/L isoproterenol (Sigma) alone, 20 μmol/L Mn (III) tetrakis (4-benzoic acid) porphyrin chloride (MnTBAP) alone, 20 μmol/L JNK inhibitor II (Calbiochem) alone, 50 μmol/L isoproterenol with 20 μmol/L MnTBAP, or 50 μmol/L isoproterenol with 20 μmol/L JNK inhibitor II. Twenty-four hours after treatment, we determined the viability of cells using trypan blue staining.

Statistics

Results are shown as means±SEM. Statistical analyses were performed by using Statcel 2 software (OMS Publishing Inc, Tokorozawa, Japan). Comparisons between 2 groups were performed using the Student *t* test. One-way ANOVAs with Bonferroni's post hoc test were used for multiple comparisons, and 1-way ANOVAs on ranks were used for multiple comparisons between normalized data. A probability value of <0.05 was considered statistically significant.

Results

Activation of the IKK/NF-κB Pathway in the Pathogenesis of Pressure Overload–Induced Cardiac Remodeling

First, we examined whether the IKK/NF-κB signaling pathway is activated during pressure overload–induced cardiac remodeling. Ten-week-old C57Bl/6J mice were subjected to pressure overload by means of TAC. We performed an in vitro kinase assay to assess the activity of the IKK complex using IκBα as the substrate. The IKK activity in hearts was elevated in response to pressure overload (Figure I, A, in the Online Data Supplement, available at http://circres.ahajournals.org). We subjected nuclear proteins to EMSA for NF-κB DNA-binding activity. We observed increased formation of DNA-protein complexes after TAC (Online Figure I, B). The specificity of NF-κB–binding activity was confirmed by the addition of a 100-fold excess of either unlabeled NF-κB or SP-1 consensus oligonucleotides to the EMSA reaction. Anti-p50 and anti-p65 subunit antibodies supershifted the major NF-κB–binding complex. Furthermore, immunohistochemical analysis for p65 subunit of NF-κB showed the increase in nuclear accumulation of p65 in response to pressure overload (Online Figure I, C). These findings indicate that pressure overload activates the IKK/NF-κB signaling pathway.